FIRST PRINCIPLE STUDY: ADSORPTION OF MOLECULAR HYDROGEN SULPHIDE ON GOLD CLUSTERS

A Dissertation
Submitted to the African University of Science and Technology
Abuja-Nigeria
in partial fulfilment of the requirement for:

MASTER OF SCIENCE DEGREE IN CONDENSED MATTER PHYSICS

By
IGUMBOR EMMANUEL
Reg no: 40016

Supervisors:

Prof Sandro Scandolo
and
Dr. Somesh Kumar Bhattacharya

November 2009

Dedication

This Thesis is dedicated to the Lord God Almighty.

Acknowledgement

I want to thank my supervisors Prof. Sandro Scandolo and Dr Somesh Kumar Bhattacharya for their immensely support and guidance, their contributions, suggestions and constructive criticism which helped me a great deal in accomplishing this great task during my thesis work at The Abdul Salam International Centre for Theoretical Physics ICTP.

I will like to thank the provost of African University of science and Technology Prof C. E. Chidume and the president Prof Hilary Inyang for their support morally, financially and academically towards the success of my programme in Africa University of Science and Technology Abuja. I want to specially thank Dr Karl Voltaire and Dr Boubou Cisse, who were the first leadership I met in Africa University Of Science and Technology for the care and love towards me and their wonderful advice which had help me in my career pursuit.

I will like to thank my fellow students of African University of science and Technology, my friends I met at ICTP, members of the church in Trieste for their moral, religious support and encouragement given to me during the period of my programme in AUST and ICTP.

Furthermore, I will like to express my profound gratitude to my parents Evang and Mrs M. A. Igumbor, for their parental care, support and love towards me during my course in AUST. My brothers and sisters are not left out, their support helped me in achieving this goal my spiritual fathers for all that they have contributed and my lovely friends Brenda Havbehron and

Atiso Domefafa Clement for their support during my study time.

Finally I will give all praise and adoration to the Almighty God for all that He Has done for me, during my course work in AUST and my stay in Trieste Italy.

IGUMBOR EMMANUEL

Contents

List of Figures

List of Tables

1

Abstract

We present theoretical results of the study of H_2S adsorption on gold cluster $Au_n(n = 1, 5)$ using density functional theory with Perdew-Burke-Ernzerhof (PBE) exchange-correlation energy functional. Minimum energy structures of the gold cluster along with their isomers are considered in the optimization process. H_2S molecule is observed to adsorb on to the gold cluster. However, the adsorption energy decreases with increasing cluster size. The structure of the gold clusters are similar before and after adsorption of H_2S molecule. The structure of gold cluster remain planar. The adsorbed molecule get adjusted in a way that their center of mass lie on the plane of the gold cluster. The adsorbed molecules get attached to a single gold atom and there is no preference to get adsorbed in between the gold. H_2S dissociation is not favoured on the Au clusters.

Chapter 1

INTRODUCTION

1 Introduction

Finite gold clusters and gold-containing nanometer-sized structures are currently being investigated because of their applications in a wide variety of areas, including medical science[1], molecular electronic devices[2-4], catalysis[5-7] and chirality of nano structures[8,9]. The structural and electronic properties of gold clusters and their compounds have been studied using various theoretical and experimental methods. It is also noted that nano size noble metal clusters and compounds have been attracting attention not only in areas of medicine, catalysis, but also for fabrication of nano devices and other applications due to their unique physical and chemical properties which depend strongly on cluster size[10,11].

Nano sized gold clusters have been studied as a new kind of catalyst to reduce air pollution[12,13]. The free and supported gold clusters can efficiently catalyze the CO oxidation reaction at low temperatures. Au_8 is found to be the smallest catalytically active cluster. The adsorption properties of NO molecule on small gold clusters have been studied theoretically as well as experimentally in order to understand the mechanism of catalysis. Hakkinen *et al.*[10] investigated the atomic and electronic structures of the neutral and anionic Au_{2-10} clusters using density functional theory (DFT) with the generalized gradient approximation GGA. They found two-dimensional (2D) structures up to seven atom for neutral clusters and six atom for anionic clusters.

There are several literatures available on Au surfaces and cluster. Wang *et al*[14], have reported local density approximation LDA based DFT studies of neutral $Au_n(n = 2 - 20)$ clusters and found two dimensional structures up to six gold atoms. On the other hand, two dimensional structures are found by Fernandez *et al.*[12] up to 12 atoms in the anionic, 11 atoms in the neutral, and 7 atoms in the cationic clusters in the study of the electronic and structural properties of the noble metal clusters Cu, Ag, and Au in their neutral and charged states. DFT study predicts that all Au_n(n= 1-6) clusters with different charged states adsorb NO molecule where Au_3^- cluster shows least stability. Laser-ablated gold clusters react with the NO molecule, in excess argon and neon, yielding the neutral nitrosyl complexes AuNO and $AuNO_2$ as the main product. Varganov *et al*[15], have studied the reaction of molecular hydrogen with the dimer and trimer gold clusters using DFT, second order perturbation theory MP2, and coupled cluster (CCSDT) methods. They report that up to two H_2 molecules easily bind to neutral Au_2 and Au_3 clusters but molecular hydrogen does not form stable complexes with Au_2^- and Au_3^- clusters. The preference of two dimensional structures in Au clusters has been attributed to the existence of strong relativistic effects, which enhances the s-d hybridization by shrinking the size of the 6s orbitals. Pyykko[16] has explained the large relativistic effects for high Z elements due to interacting relativistic and shell structure effects, higher shells being orthogonal to the lower ones with same "l" value. Study of ion mobility measurements[17] on gold cluster cations Au^+ for n > 14 show planar structure up to the seven atom gold cluster.

Calculations on the interaction of sulfur containing molecules with gold clusters have been carried out to understand the chemistry at the gold-sulfur interface. To investigate the chemisorption of alkane thiolates on gold surfaces, Sellers *et al.*[18] studied $Au_{16}SCH_3$ cluster to be used as a model for the thiolate-Au(111) surface. In their work the geometry was optimized by varying the AuS distances and the AuSC angle only. A similar model calculation was also performed by Beardmore *et al.*[19] for $Au_{17}SCH_3$ and Majumder *et al.*[20] for $Au_{24}SCH_3$. In both cases, the emphasis was to understand the chemical interactions at the gold-sulfur interfaces. Thiol-terminated molecular diodes interacting with the noble metal clusters (Cu, Ag, and Au) have been investigated[17] using DFT, which have particular implications in the field of nano-electronics[21-22].

Heavy metal chalcogenide clusters are widely used in catalysis, photo-catalysis, and micro-electronics. They also play an important role in some luminescent properties, for example, as photosensitive and nonlinear optical materials. Gold sulfide, in bulk, is a semiconductor with intermediate band gap and has mixed ionic and covalent bonding character[23].

To utilize the properties of gold clusters, it is necessary to avoid their coalescence. Molecules containing sulfur atoms are often used as surfactants, since they form particularly stable gold nano-clusters due to the strength of the gold- sulfur bond[24]. The interaction of H_2S with gold and silver can also serve as a simple model system for understanding the self-assembly of alkane thiols (RSH) on noble metal surfaces[25]. The adsorption of H_2S on

a number of metal surfaces, including Ni(100)[26], Cu(100)[27], Au(110)[28], Au(100)[29], and Ag(111)[30] have been reported. A variety of techniques, including low energy electron diffraction, temperature programed desorption, high resolution electron energy loss spectroscopy, x-ray photo-emission spectroscopy, ultraviolet photo-emission spectroscopy, near-edge x-ray adsorption fine structure, and scanning tunneling microscopy have been used to characterize such surfaces. In most cases, dissociation of H_2S and formation of a chemisorbed sulfhydryl SH species is observed at low coverage and low temperature below 170 K; the major exception being gold and silver surfaces.

In order to design new molecular devices it is extremely important to understand the chemical interactions of these molecular systems at the junctions. Several theoretical investigations, describing the adsorption of alkane thiols on gold surfaces, represented by cluster models, have been reported. Pioneering calculations on adsorption of SCH_3 on Au_{16}, Au_{17}[31] and Au_{24}[24] are carried out with an emphasis to understand the chemistry at the gold-sulfur interface. It is found that the geometries of the atoms beyond the terminal sulfur are virtually unaffected even after strong adsorption. Remarkably little work has been reported for H_2S with gold clusters. In this work, we report a theoretical study of the adsorption of H_2S molecules on small neutral gold clusters, $Au_n (n = 1 - 5)$ and compare our calculations with available results. The adsorption of molecular hydrogen sulphide on gold cluster was performed using DFT calculation, in which the minimum energy for adsorption of molecular hydrogen sulphide on the various cluster was reported. We analyzed our results with the density of state to have a deep insight of the

electronic states.

This work is organized as follows. In chapter 2 we review the fundamental theoretical tools used in the calculation and the computational details of our work. In chapter 3 we present and discuss the results of this work and finally, in chapter 4, we present a brief summary of our results and conclusion.

Chapter 2

METHODOLOGY

2 Density functional theory

In this chapter we will discuss briefly Density functional Theory used to study the ground state geometrical and electronic properties. There are several extensive discussions in the literature[32-36] on the foundations of DFT and the approximations which are used in its implementation. Here we will be content to present and describe the formalism and to investigate the use of pseudo potentials in DFT. First it is necessary to establish some important notation that we help us understand this work properly. We consider a periodic system with atoms at positions R + r, where R is a Bravais lattice vector locating a unit cell of the crystal and r is a basis vector giving the positions within the unit cell. The Hamiltonian of the system is given by

$$H = -\sum_{i=1}^{N} \frac{1}{2m}\nabla^2 + \sum_{i=1}^{N} V_{ion}(r_i) + \frac{1}{2}\sum_{i\neq 1}^{N} \upsilon(r_i - r_j) + V_{I-i} \qquad (1)$$

which describes N electrons at positions r_i interacting via the Coulomb potential $\upsilon(r) = \epsilon^2/|r|$ and moving in the potential of the static ions given by

$$V_{ion}(r) = \sum_{m,s} V_{ion}^{(s)}(r - R_m - r_s) \qquad (2)$$

in terms of ionic potentials $V_{ion}^{(s)}$. The ion-ion repulsion is given by

$$V_{I-i} = \frac{1}{2}\sum_{mm'ss'} \frac{Z_s Z_{s'}\epsilon^2}{|R_m + r_s - R_{m'} - r_{s'}|} \qquad (3)$$

where the prime indicates the $m = m'$, $s' = s$ term is to be omitted from the summation. We will use throughout this chapter Rydberg atomic

units $\hbar = 1$, $2m = 1$, $e^2 = 2$, wherein distances are measured in Bohr and energies in Rydberg. The e^2 and $2m$ factors will often be retained in explicit expressions for energies and potentials for clarity. The first three terms in 1 are often lumped together as the electron energy operator H^{el}.

Obviously all electronic properties of this system are functionals of the ionic potential $V^s{}_{ions}$ since only fundamental constants appear elsewhere in H. A central result of DFT is that the ground state electronic energy E^{el} of the system is given by

$$E^{el} = T_o[n] + \int V_{ion}(r)n(r)dr + E_h[n] + E_{xc}[n]. \tag{4}$$

Here $T_o[n]$ is the kinetic energy of a system of non-interacting electrons with density n_r, E_h is the classical interaction energy and

$$E_h[n] = \frac{1}{2}\int\int n(r)\upsilon(r-r')n(r')drdr' \tag{5}$$

is the remaining energy, termed the exchange-correlation energy, which is a functional of n alone.

A second result of DFT is the E^{el} is minimized, with respect to number-conserving variations of the density, by the true ground state density $\mathrm{n}_o(r)$,:

$$\delta(E^{el}[n] - \mu\int n(r)dr) = 0 \tag{6}$$

$$\frac{\delta E^{el}[n]}{\delta n(r)}|_{n=n_0} = \mu \tag{7}$$

where μ is the (constant) chemical potential of the electronic system. One can reduce the many body Hamiltonian to a set of Kohn-Sham equations

[4-8], which are single particle equations to be solved self-consistently:

$$h\Psi_i(r) = (-\frac{1}{2m}\nabla_i^2 + V_{eff}(r;n))\Psi_i(r)i = \epsilon_i\Psi_i(r) \tag{8}$$

$$V_{eff}(r;n) = V_{ions}(r) + V_h(r;n) + V_{xc}(r;n), \tag{9}$$

$$n(r) = \sum_{i=1}^{N} |\Psi_i^2|^2 \tag{10}$$

where Ψ are orthonormal eigenfunctions and ϵ_i are the associated eigenvalues of the one-body Hamiltonian h in Eq8, and the sum in Eq10. extends over the N lowest eigenvalues. The Hartree and exchange-correlation (XC) potentials are given by

$$V_h(r;n) = \int \upsilon(r-r')n(r')dr' \tag{11}$$

$$V_{xc}(r;n) = \frac{\delta E_{xc}[n]}{\delta n(r)} \tag{12}$$

This Kohn-Sham procedure introduces a one-body Hamiltonian which has the natural interrelation, but without formal justification, as describing an electron in the effective mean field V_{eff} in fact, the non-interacting kinetic energy $T_o[n]$ was introduced into the expression (4) as a single particle kinetic energy term ($-\frac{1}{2m}\nabla^2$) would appear in Eq 8. In spite of the fact that DFT itself assigns no formal interpretation to Ψ_i and ϵ_i it has been recognized for decades that the eigensolutions of the related Hartree-Fock-Slater equation closely resemble single particle excitation energies and wave functions in many systems. This interpretation can be shown [8] to follow from Greens function theory, which provides a formalism for single particle excitations. Excitations are described by an equation analogous to Eq 8, with

the complication that V_{eff} is replaced by a non-Hermitian energy-dependent self-energy see Pickett [36]. This self-energy, however, is often similar in its effect to V_{eff}, hence the close resemblance of Ψ_i and ϵ_i to excited state properties of the many body system. Although this interpretation will not be relied on in this review, $h\Psi_i$ and ϵ_i will be referred to as the single electron Hamiltonian, wave function and eigenvalue, respectively.

One point which is of concern here is that the potential imposed on the electrons in DFT, denoted V_{ion} in Eq 1, is a *local function* (simple real function of r). This is a requirement for the formal validity of DFT - the external potential must be local. The nuclear potential,

$$V_{ion}^{(s)}(r) = \frac{Z_s \epsilon^2}{|r - R_s|} \tag{13}$$

satisfies this requirement trivially. As we will discuss below, there have been extensive, very successful applications of DFT in which V_{ion} is *taken to be a non-local pseudo potential*. Somewhat surprisingly, there has been very little justification of this procedure, except in terms of its results.

2.1 Validity of non-local potentials

In density functional theory Gilbert[37] considered non-local potentials in the context of DFT and concluded that there is no DFT in such a case. He established rather that for a general non-local external potential of the form $V_{ext}(r, r')$, the density matrix $\mu(r, r')$ is analogous to the density in DFT. There is a density matrix functional theory, and a Kohn-Sham-like Schroedinger equation for the orbitals and eigenvalues, but in addition to the non-local external potential the exchange-correlation potential is also non-

local. Berrondo and Goscinski[38] and Levy[39] have also investigated the introduction of non-local potentials in DFT and come to similar conclusions. In principle, DFT is not formally valid with non-local potentials. However, Gilberts conclusion allows it to be generalized to an analogous density matrix functional theory with a *non-local exchange-correlation potential* $V_{xc}(r, r')$,

$$V_{xc}(r, r' : \mu) \equiv \frac{\delta E_{xc}}{\delta \mu(r; r')} \tag{14}$$

occurring in the Kohn-Sham equations. (Gilbert notes that there are formal difficulties in proving the existence of this functional derivative, The result then is that the use of non-local potentials is equally as valid as local potentials within current applications of DFT.

2.2 Validity of frozen core approximation in total energies studies

Another point of concern here is the validity of the pseudo potential approximation - that is, the frozen core ansatz - in carrying out density functional studies of energetics. As described in section 1, the pseudo potential is defined by the condition that it reproduce one electron properties (eigenvalues and wave functions) accurately, but no condition involving energetics is imposed. It is less obvious then that pseudo potentials will be successful in such applications, even if one restricts the use to situations where core overlap is negligible.

This concern was noted by Janak [40] in the course of comparing the energies of competing crystal structure using all-electron methods. According

to the viral theorem, the total energy is equal to the negative of the kinetic energy K. Janak used the Xa approximation for the XC potential, where $V_{xc}(r)$ is proportional to $n^{\frac{1}{3}}(r)$, for which he reasoned that the XC contribution to K vanishes. Then K can be partitioned into core and valence parts K_c, and K_v, given by

$$K_c = \sum_c \int (-\frac{1}{2m}\nabla^2)\Psi_c d^3r \tag{15}$$

$$K_v = \sum_v \int (-\frac{1}{2m}\nabla^2)\Psi_v d^3r \tag{16}$$

Several detailed studies since that time have confirmed, however, that the pseudo potential method does predict structural energies properly, except in certain cases where very polarizable semi core states contribute to bonding in the crystal. Von Barth and Gelatt[41] resolved this paradox by an unorthodox application of density functional theory. They first dramatized the paradox by noting that the core kinetic energy of Mo changes by $5eV$ in forming the crystal, and also that the change in K_c, between bcc and fcc Mo is $2.7eV$ compared to the total energy difference of $0.5eV$ per atom. These facts appear to invalidate the pseudo potential approach and the frozen core assumption which underlies it. The core pseudo potential is considered to be a fixed quantity, unchanging when an atom moves to a different environment. This transferability precept appears to rely on the assumption that different environments will not alter the core and its properties, and Janaks all-electron calculations show this assumption to be inadequate.

Von Barth and Gelatt [41] approached this problem by defining an energy functional of the core and valence densities $n_c(r)$ and $n_v(r)$ separately. Al-

though the last three terms of 4 can be generalized trivially by the replacement $n(r) \longrightarrow n_c(r) + n_v(r)$, the kinetic energy term is less straightforward. Nevertheless, they established the existence of a functional $T_o[n_c, n_v]$ which is not equal to $T_o[n]$ which is sufficient to describe the system to second order in $n_v - n_v^o$ and $n_c - n_c^o$ around the physical density $n^o = n_c^o + n_v^o$. Using this functional they derived an expression for the error in total energy made by using the frozen core approximation,

$$\delta E_{fc} = \int [\rho_c^{fc}(r) - \rho_c(r)][V_{eff}^*(r) - V_{eff}^{fc}(r)]d^3r \tag{17}$$

Here ρ_c^{fc} is the frozen core density, $V_{eff}^*(r)$ is an effective potential (see 9) which will produce ρ_c^{fc} and

$$V_{eff}^*(r) = V_{eff}(r; n_c^{fc} + n_v^*) \tag{18}$$

Eq 18 is the effective one-body potential in the self-consistent frozen core calculation, for which the valence density is n_v^*. This energy correction is second order in the difference between frozen core density and true core density, the result which is essential to the validity of the frozen core approximation.
Calculations performed by von Barth and Gelatt confirmed both the second order nature of δE and the accuracy of Eq 17. They found that a simple way to understand how the first order terms vanish is to consider the relaxation of the frozen core approximation in two stages: first let the core relax in fixed valence density n_v^*, then let the valence electrons relax with this new (relaxed) core held fixed. The stationarity of their functional with respect to core and valence densities separately guarantee that the energy change is second order in each stage. They concluded that total energy errors in the frozen core approximation should typically be no more than $\sim 0.1eV$; subsequent studies suggest it is an order of magnitude better than this figure, as

it must be useful in predicting pressure-driven structural transformations.

Finally one is led to Janaks argument - what was overlooked in his analysis? In his analysis he was relating energy differences to kinetic energy differences using the viral theorem. There are two weaknesses in applying this approach to *approximate densities*. First, the error in the kinetic energy is *first order* in the error in density, which makes this an unacceptable method for estimating errors. Second, and specific to the frozen core situation, is that the viral theorem is not satisfied by the frozen core approximation. As a result, energy differences which are actually of second order appear to be of first order.

2.3 Local Density Approximation

One of the most widely used approximation for the exchange energy is Local Density Approximation: which is given by

$$E_{xc}^{LDA}[n] = \int n(r)\epsilon_{xc}(n(r))dr \tag{19}$$

where $\epsilon_{xc}(n)$ is taken to be the exchange and correlation energy per particle of a uniform electron gas whose density is n. This has been accurately calculated by using Monte Carlo simulation [42] and parameterized in order to be displayed in an analytic form [43]. By construction this approximation yields exact results if the density of the system is uniform, and should not be very accurate for those systems whose density is highly non-homogeneous, as for example for atoms and molecules. However, it turns out to work better than expected for a wide range of materials. In molecules, for example, the LDA usually overestimates the binding energies, but it yields in general good

results for equilibrium distances and vibrational frequencies.

Within this approximation, the exchange and correlation part of the KS potential is

$$V_{xc}^{LDA} = \frac{\delta E_{xc}^{LDA}[n]}{\delta n(r)} = \epsilon_{xc}(n(r)) + n(r)\frac{d\epsilon_{xc}}{dn(r)}$$

(20)

But $E_{xc}^{LDA}[n] \neq \int V_{xc}^{LDA} n(r) dr$

2.3.1 Plane-Wave Pseudo potential Method

In this method, the plane wave basis set u_{nk} can be written as:

$$u_{nk}(r) = \sum_{G} e^{iG.r} c_{nk}(G) \tag{21}$$

where G is a reciprocal lattice vector.

The KS eigenvalues have no physical meaning but it it has been shown that their collection in reciprocal space resembles the band structures of solids. The number of PWs used in Eq.21 is determined by the condition

$$|k + G|^2 \leq E_{cut} \tag{22}$$

Eq. 22 defines a sphere in reciprocal space whose radius is $\frac{E_{cut}^{\frac{1}{2}}}{\Omega_{BZ}^{\frac{1}{3}}}$ where Ω_{BZ} is the volume of the BZ. The number of PWs inside this sphere is then roughly

$N_{pw} \approx \frac{4}{3\Omega_{BZ}} E_{cut}^{\frac{3}{2}}$ which, for a fixed cutoff energy and then a fixed accuracy in the description of the KS wave-functions, is linear in the volume of the unit cell. Given a fixed accuracy the number of PWs needed depends on

the shape of the KS orbitals. This depends on the details of the electronic structure which must be described.

2.3.2 Pseudo potential approximation

The $c_{nk}(G)s$ defined in Eq.21 are the Fourier components of the atomic orbitals. Due to the localization of the core electrons and to the rapid oscillations in the core region of the wave-functions which describe the valence electrons, the number of PWs needed, even for a simple calculation, is huge. We need approximations to avoid this problem. The first idea is to disregard the core electrons because they do not participate in the chemical properties of matter, at least until their binding energy is much higher than the energy involved in the chemical properties one wants to study. So one freezes them around the nuclei and redefines the system as if it was formed by ions plus valence electrons. We are left with the second problem, how to deal with the oscillations in the core region of the valence wave-functions, due to the orthogonalization to the core wave functions. The solution to this is the introduction of a pseudo potential (PP) which substitutes the ionic Coulomb potential in such a way that the valence pseudo eigenvalues are the same as the all electron (AE) ones and the pseudo wave functions coincide with the AE ones from a fixed core radius on, and are as smooth as possible below the core radius, with the only constraint to be normalized (norm-conserving (NC) pseudo-potentials). An ionic potential, valence wave function and corresponding pseudo potential and pseudo wave function have been illustrated in so many literatures.

From the various literature, we discovered that the pseudo wave function

and all electron wave function (AE) and corresponding pseudo potential and ionic potential are identical outside the cutoff radius rc. Near the core region there is rapid oscillation of AE wave function while pseudo wave function is smooth. To satisfy this requirements the PP usually must be angular momentum dependent, i.e. pseudo-wave-functions corresponding to different angular momenta are eigenfunctions of different potentials. However, the long range behaviour of these different potentials must resemble the true one, because above the core radius the pseudo wave-functions are identical to the AE ones. This means that the difference must be confined in the core region and then the PP can be written in the following form [44]

$$V_s^{sl}(r,r') = V_s^{loc}\delta(r-r') + \sum_{l=0}^{l_{max}} V_{s,l}^{nl}(r)P_l(r-r')\delta(r-r') \tag{23}$$

where $V_s^{loc}(r)$ is a local, long range part and approaches the AE potential above a cutoff radius r_c^{loc} , and $V_{s,l}^{nl}(r)$ are the non-local short range angular momentum dependent part, the index s refers to the atom, the superscript sl emphasizes the semi-locality (non local in angular momentum but local in r) and P_l is the projector onto the angular momentum l,

$$P_l(r,r') = \sum_{m=-1}^{l} Y_{l,m}(\theta,\Phi)Y_{l,m}^*(\theta',\Phi') \tag{24}$$

with the $Y_{l,m}$s the spherical harmonics. The quality of the PP depends on transferability properties, i.e. the capability to reproduce the AE results over a wide range of electronic configuration.

2.3.3 Ultra-Soft (Vanderbilt) pseudo potentials

The requirement of norm conservation for the pseudo-wave-functions can be a limiting factor for numerical calculations when also the valence electrons

are very localized around the nuclei. This is a particularly serious problem for first row elements, like carbon and more so for nitrogen, oxygen, and for transition metals, where the d-electrons are as localized as shallow core states but have an extraction energy which is comparable to valence energies, and for this reason cannot be excluded from the calculation. If this is the case the utilization of NC pseudo potentials requires huge PWs basis sets to achieve an acceptable accuracy. In a work published in 1990 Vanderbilt [45] showed that, introducing a generalized formalism, the norm conservation constraint can be removed. In this way one can construct much smoother pseudo wave functions, with the only constraint of matching the AE ones at and above a fixed core radius. The price to pay for having so smooth pseudo-wave-functions is the introduction of a new generalized formalism. Due to the fact that the pseudo wave functions are no more normalized, the charge density has to be restored by adding an augmentation part. More details of the Ultra-soft Pseudo-potential method can be found in [45].

2.3.4 Forces

The knowledge of the forces among the atoms is a fundamental ingredient when ever one is interested in optimizing geometric structures, or studying the dynamical evolution of the system. Ionic forces are the energy derivative with respect to the ionic displacements. Using the Hellmann-Feynmann theorem [46], it is possible to obtain the forces. The Hellmann-Feynmann theorem is a general result which applies for the energy derivative with respect to an arbitrary parameter , from which the external potential depends. In the case of forces, is the collection of the ionic positions. The energy

derivative with respect to can be written as

$$\frac{dE}{d\lambda} = \int n_\lambda \frac{dV}{d\lambda} \tag{25}$$

which only requires the knowledge of the actual density. Therefore, with only one self-consistent calculation, one has the total energy and the forces on the atoms.

2.4 Fermi Energy

The Fermi energy, of a substance is a simple concept with far reaching results. It is a result of the Pauli exclusion principle when the temperature of a material is lowered to absolute zero. By this principle, only one electron can inhabit a given energy state at a given time. When the temperature is lowered to absolute zero all of the electrons in the solid attempt to get into the lowest available energy level. As a result, they form a sea of energy states known as the Fermi Sea. The highest energy level of this sea is called the Fermi energy or Fermi level. At absolute zero no electrons have enough energy to occupy any energy levels above the Fermi level. In metals the Fermi level sits between the valence and conduction bands. The size of the so called band gap between the Fermi level and the conduction band determines if the metal is a conductor, insulator or semiconductor.

Once the temperature of the material is raised above absolute zero the Fermi energy can be used to determine the probability of an electron having a particular energy level.The probability that an energy state is filled by an

electron depends on the Fermi energy is given as

$$f(E) = \frac{1}{\epsilon^{\frac{(\varepsilon-\varepsilon_f)}{KT}} + 1} \tag{26}$$

2.5 Density of states

The Density of states which is the distribution of the energy levels, is the number of states with energy between ϵ and $\epsilon + \Delta\epsilon$, where $\Delta\epsilon$ is very small compared to ε_f. Given the total number of states with energy below ϵ as

$$N = \frac{V}{3\Pi^2}\left(\frac{2me}{\hbar^2}\right)^{\frac{3}{2}} \tag{27}$$

Therefore the energy density of orbitals is

$$\frac{dN}{d\varepsilon} = \frac{V}{2\Pi^2}\left(\frac{2m}{\hbar^2}\right)^{\frac{3}{2}} \varepsilon^{\frac{1}{2}}. \tag{28}$$

The results shows that the density of states increases parabolically with energy, this implies that when the energy increases, the number of states with similar energies increases. The density of states at the Fermi level(the number of electrons energetically close to unoccupied states) is an important parameter in the free electron model, since only electron in these states are able to participate in dynamic processes such as electronic conduction.

2.6 Computational Details

All calculations presented in this work was done using the plane-wave expansion method as implemented in the *ab initio* Quantum espresso-4.1[16]. Quantum ESPRESSO which is an integrated suite of computer codes for electronic-structure calculations and materials modeling at the nano scale. It is based on density-functional theory, plane waves, and pseudo potentials

(both norm-conserving and ultra soft).

The electron-ion interactions were described by ultra soft pseudo potentials[17]. we employ Perdew-Burke-Ernzerhof (PBE) for the exchange-correlation energy functional and a convergence criterion of $10^{-4}eV$ for the total electronic energy. A cubic super cell of size of 20 was taken and periodic boundary conditions was imposed. The clusters were perfectly positioned at the center of the cell. The size of the cell is found to be sufficient to avoid any spurious inter-cluster interactions.

Structural optimizations were perform for each A_u cluster, and have obtained, for each cluster and cluster adsorbate, multiple isomers. It may be mentioned that starting configurations considered for the adsorption also included several isomers of the bare clusters to find the minimum energy geometry of the complex.

The cutoff energy for the plane-wave basis set up appropriately for the adsorption of H_2S molecule. The gold clusters and adsorbate molecules H_2S were separately optimized before commencing the optimization process for adsorption.

The convergence threshold for the force and total energy was set to $1.0D-5$ and $1.0D-4$ respectively, the mixing beta was set to 0.6. The cutoff energies for the plane-wave basis set was also set upfor simulating the bare molecules H_2S. The calculated $H-H$ and $S-H$ average distances in the optimized

geometry of H_2S molecule were 1.93 and 1.34 , respectively, and the H_2S average bond angle is 91.8 in agreement with experimental results[19].

For simulating the adsorption process, the H_2 and H_2S molecules were placed, respectively, at a distance of 2.50 and 3.40 from the gold cluster. These distances are quite large as compared to the $Au-H$ distance[6] and the $Au-S$ distance[20] calculated earlier and guarantee free movement of the molecules in the cell before they get adsorbed. In all the calculations for gold clusters and absorption of hydrogen sulphide, the kinetic-energy cutoff was set to 35Ry the charge density cutoff was also set to 270Ry while the degauss was set to 0.01. Different orientations of the molecule with respect to gold cluster were considered for optimization and the molecules and the gold clusters are allowed to relax freely. Based on the optimized geometries, we calculate the binding energy, defined by the following equation:

$$BE = nE[Au] - E[Au_n] \tag{29}$$

The Adsorption energy was calculated using this equation

$$E_{ads} = E[Au_n + H_2S] - (E[Au_n] + E[H_2S]) \tag{30}$$

The density and projected density of states were calculated for the various gold clusters and the adsorbed molecule, in all the DOS and proj-dos calculations, the ngauss was set to 0, the degauss was set to 0.01 while the minimum and maximum energy varies.

Chapter 3

RESULTS AND DISCUSSION

3 General consideration

In this chapter, we present the main findings of our work. We discuss the density functional theory (DFT) based study of molecular adsorption of H_2S on different Au clusters. We have considered Au_n(n=1-5) and attached H_2S to the clusters. First we relaxed H_2S to determine the equilibrium geometry. Then we study the adsorption of H_2S to Au clusters. The chapter is divided in the following sections:

1. The study of Au_n cluster
2. The study of H_2S adsorption on Au_n clusters

3.1 Au clusters.

In this section we show the results of the DFT calculations of the various gold clusters. Table 1 shows the results of the DFT calculation of Au clusters, it was obvious that the binding energy increases with the size of the cluster. Au has no binding energy and bond length because it is a single atom. The bond angle of the gold trimer was 60°, this shows that they are highly symmetric.

(a) Au_2 (b) Au_3

Figure 1: *Relaxed Gold clusters* Au_2 *and* Au_3

(a) GM (b) LM

Figure 2: *Relaxed Gold clusters* Au_4

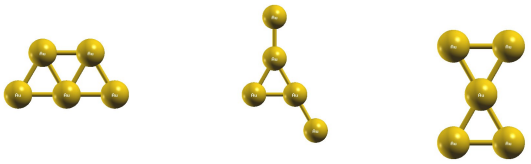

(a) GM (b) FLM (c) SLM

Figure 3: *Relaxed Gold cluster* Au_5

Table 1: *Gold Cluster 1-5*

No	Gold Atom(s)	Binding Energy eV	Au-Au Distance(Å)
1	Au	-	-
2	Au_2	2.55	2.54
3	Au_3	3.82	2.68
4	Au_4 (GM)	6.66	2.69
5	Au_4 (LM)	6.58	2.63
6	Au_5 (GM)	8.98	2.69
7	Au_5 (FLM)	8.21	2.63
8	Au_5 (SLM)	8.55	2.66

From our DFT calculation of Au_4 with different geometries, we discovered that the minimum energy configuration is called the global minimum (GM), and energetically the next higher configuration is called the local minimum (LM). This is as a result of the difference in shape. From figure 2(a) we see that GM is highly symmetric than LM, this accounted for the variation in the minimum energy.

The results of the DFT calculation of Au_5 of different geometries see (figure 3) shows that it has global, first local and second local minimum with the global minimum (GM) having the highest binding energy. As in the case of Au_4, the global minimum of Au_5 is highly symmetric compared to FLM and SLM.

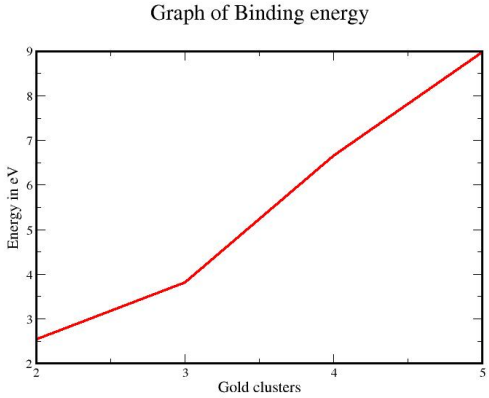

Figure 4: *The plot of Binding energy of Gold cluster with minimum energy Vs number of gold atoms*

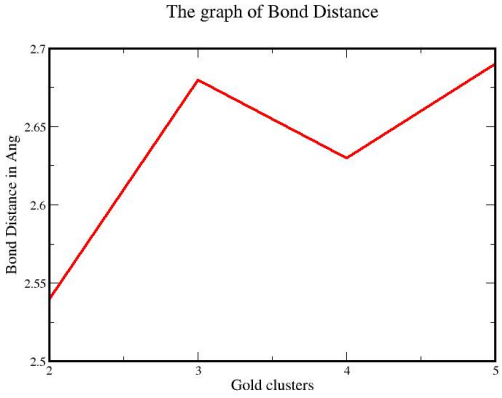

Figure 5: *The plot of Au-Au bond length for minimum energy configurations Vs number of gold atoms*

3.1.1 Electronic properties DOS

The Density of states (DOS) of the various gold clusters where calculated. Below we show plot for DOS of Au_3 and Au_5

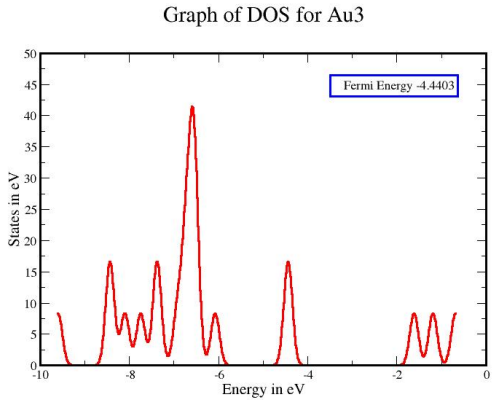

Figure 6: *Density of state graph of* Au_3

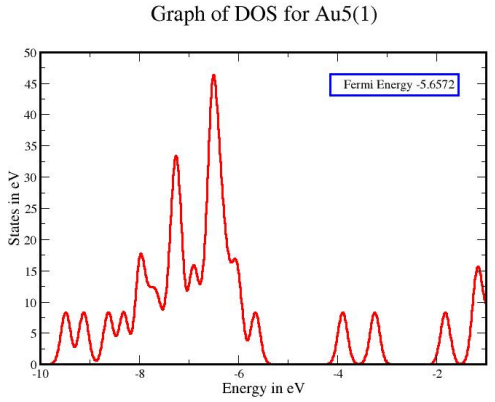

Figure 7: *Density of state graph of* Au_5

3.1.2 Projected Density of state

The projected density of states for the various gold clusters were calculated, in some of the calculation we discovered that there was overlapped in the orbitals. Below are the plot for gold cluster 5 and Au-d. The d orbitals are located near the Fermi level and these are responsible for bonding as we will see in a later section.

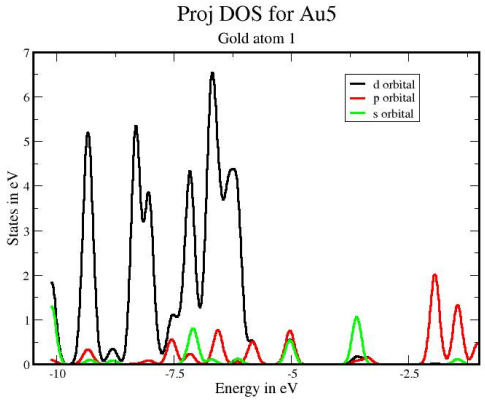

Figure 8: *Projected Density of state graph of* Au_5 *(gold atom 1)*

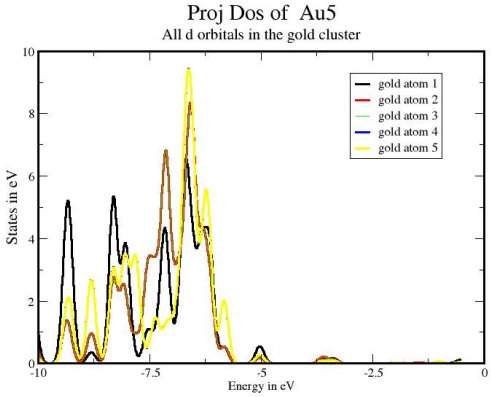

Figure 9: *Projected Density of state graph of Au_5-d orbitals*

3.2 Molecular Hydrogen and Hydrogen Sulphide

3.2.1 Hydrogen

From our DFT calculation, the SCF calculation of hydrogen atom was done, where we obtained the minimum energy of the single hydrogen atom to be -0.998 Ry which is in aggrement with known results 1 Ry.

3.2.2 Hydrogen Sulphide

The relaxation calculation of molecular hydrogen sulphide was carried out, the minimum energy of the system was -310.52 eV. The hydrogen sulfur distance after the relaxation was found to be 1.3 Å, and the bond angle was 91.86° in agreement with other existing results Hagos *et al*[47].

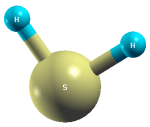

Figure 10: *Relaxed structure of Hydrogen Sulphide*

3.2.3 Electronic properties:DOS and Proj-DOS

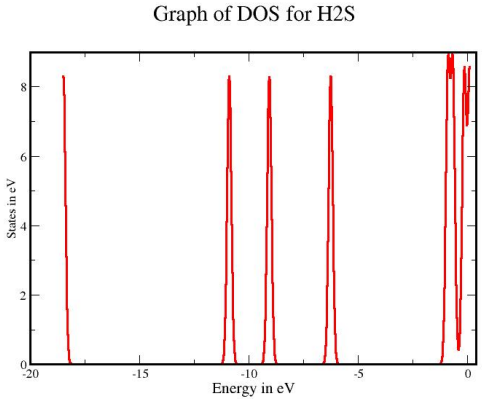

Figure 11: *DOS of H_2S*

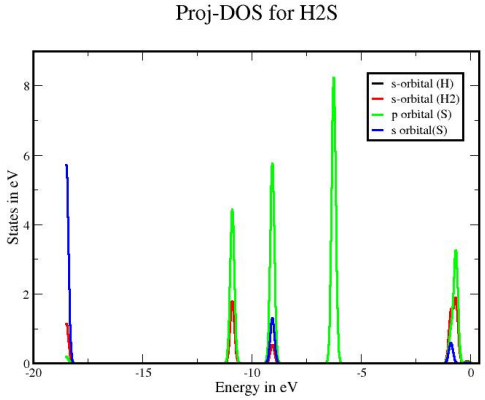

Figure 12: *proj-DOS of H_2S*

3.3 H_2S attached to Au clusters

In this section, we will show the results of the DFT calculations of the various Au clusters and its adsorbate (H_2S).

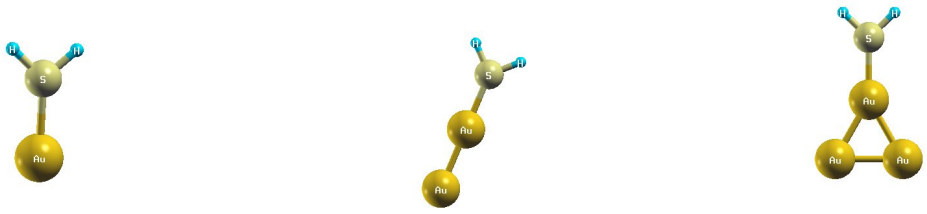

(a) AuH_2S (b) Au_2H_2S (c) Au_3H_2S

Figure 13: *Relaxed structures of Gold clusters with adsorbate*

(a) GM (b) LM

Figure 14: *Relaxed structures of* Au_4H_2S

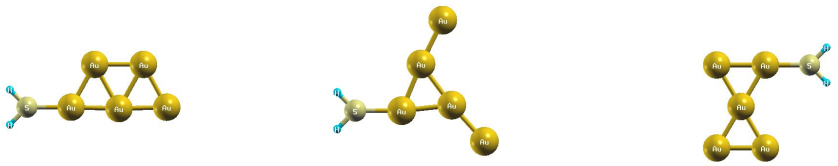

(a) GM (b) FLM (c) SLM

Figure 15: *Relaxed structures of* Au_5H_2S

From Table 2, the total energy of gold clusters when H_2S is attached to it shows a decrease with respect to the increasing size. The adsorption energy reduced with increase in the cluster size. The bond angle for H_2S before and after adsorption on Au_3 were the same. The nearest gold distance to hydrogen is 3.41 Å.

Table 2: *Summarized table of Gold Clusters 1-5 with adsorbate*

No	cluster	Adsorption Energy eV	Au-S Distance(Å)
1	AuH_2S	-0.19	2.63
2	Au_2H_2S	-0.70	2.33
3	Au_3H_2S	-0.79	2.31
4	Au_4H_2S(GM)	-0.74	2.31
5	Au_4H_2S(LM)	-0.72	2.32
6	Au_5H_2S (GM)	-0.79	2.39
7	Au_5H_2S(FLM)	-0.52	2.35
8	Au_5H_2S(SLM)	-0.33	2.41

From Table 2, we can see that the adsorption energy of the different geometries of Au_4 differs but with neglible differences. This difference was as a result of the differences in the gold clusters minimum energies, the global (GM) and local minimum (LM). The global minimum energy have the lowest total energy and the highest adsorption energy, this was as a result of the symmetric nature. It was also discovered that the bond angle for H_2S before and after adsorption on Au_4 were the same. The nearest gold distance to hydrogen was 3.51 Å, for both GM and LM, but the farthest gold atom distance to the hydrogen was different in both cases, GM was 6.09 Å, while for LM was 6.11 Å, which also contributed to the change in total minimum energy.

For Au_5H_2S, a look at fig 15 and table 2 shows clearly that there were changes, with regards to the system, this was as a result of the variations in

the gold clusters (FLM, SLM and GM) total energy before the attachment. The first Au_5H_2S (GM) have the largest bond length and absorption energy. For the three cases, the H_2S bond angle remains the same both before and after adsorption, the nearest Au atom to hydrogen atom bond length for FLM, SLM and GM are the same 3.15 Å, while the farthest Au atom to hydrogen atom bond length were 7.74, 8.70 and 7.05 Å, for FLM, SLM and GM respectively.

To conclude this section, a look at the table of different shapes of Au clusters with H_2S attached to them shows the adsorption energy to be negative, indicating that gold forms bond perfectly with hydrogen sulphide. Similar to total energy of Au clusters, the total energy of gold cluster with adsorbate decreases as the system grows. No strong change in the structural rearrangement of bare gold cluster is observed in the optimization of the Au cluster-H_2S molecule adsorption. For Au_4H_2S and Au_5H_2S, the most symmetric system has the global minimum energy.

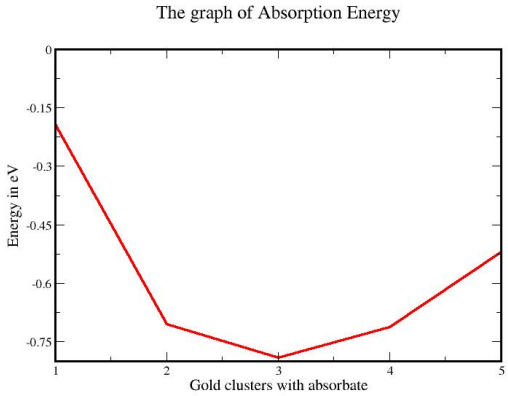

Figure 16: *The graph of Adsorption energy*

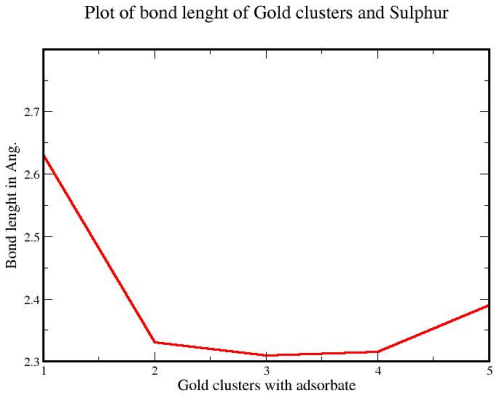

Figure 17: *The Au-S bond length*

3.3.1 Electronic properties: DOS and Proj-DOS

The Density of states of the various gold clusters and its adsorbate where calculated. below are the display of the plotted DOS for Au_2H_2S and.Au_5H_2S

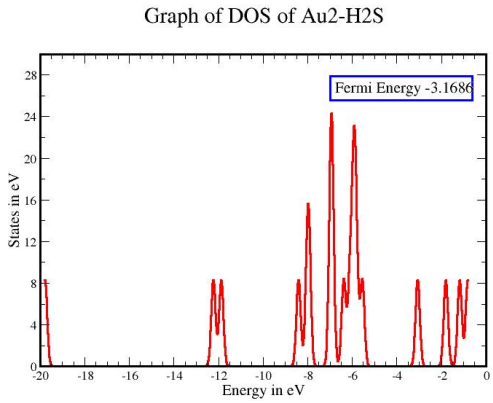

Figure 18: *Density of state graph for Au_2H_2S*

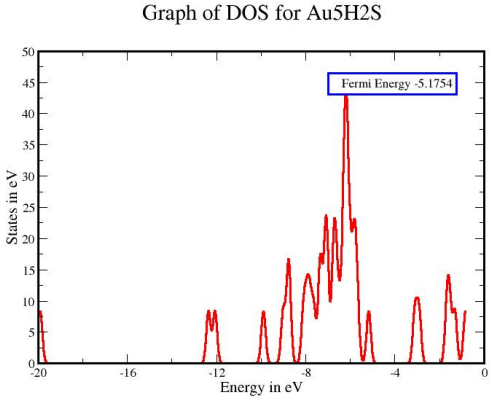

Figure 19: *Density of state graph for Au_5H_2S*

From 18 and 19, we can see that the distribution of energies or electron density is high below the Fermi energy. From 20 and 21, the projected density of states plot, we discovered that there was overlapping between the s-p and Au-d orbitals, which give rise to the strong p-d bonds.

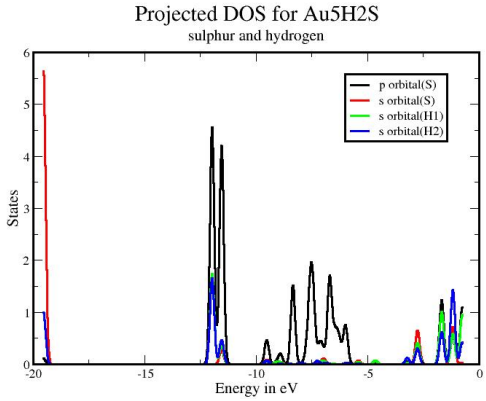

Figure 20: *Projected Density of state graph for Au_5H_2S (sulphur and hydrogen atoms)*

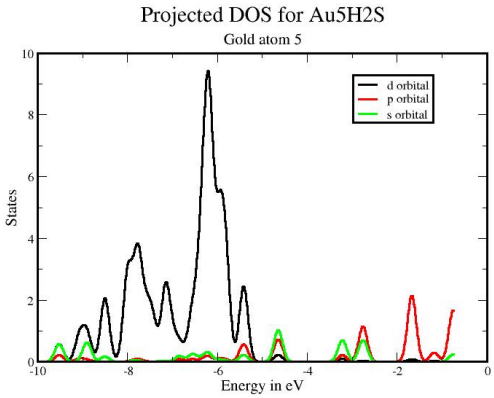

Figure 21: *Projected Density of state graph for Au_5H_2S (gold atom 5)*

3.3.2 Dissociation of H_2S on Au_n clusters

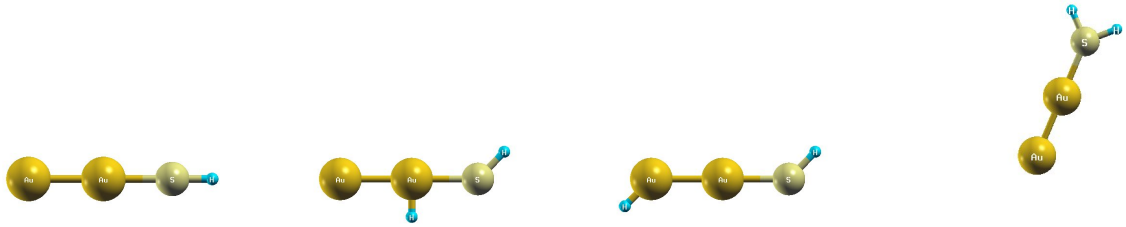

(a) Au_2HS (b) Au_2H_2S (c) Au_2H_2S (d) Au_2H_2S

Figure 22: *Relaxed structures of Gold clusters with adsorbate*

We consider different fragmentation channels and the following are our observations:

1. E[Au_2H_2S] -E[Au_2HS] - E[H] = -0.301 Ry

   From this result it is obvious that Au_2H_2S is more stable than Au_2HS + H (see figure 22(a)).

2. $Au_2H_2S \longrightarrow Au_2$-H-HS

   E[Au_2H_2S] - E[Au_2HS] - E[H] = -0.301 Ry.

   In this result, Hydrogen atom was attached to the centered Au atom (see figure 22(b)) with a distance of 1.35 Å. The minimum energy of the structure was -226.695 Ry, which is a little lower than when the hydrogen atom is attached to sulphur.

3. $Au_2H_2S \longrightarrow HAu_2HS$

   E[Au_2H_2S] - E[Au_2HS] - E[H] = -0.293 Ry.

   In this case the hydrogen atom was attached to the first Au atom (see figure 22(c)) with bond length of 1.35 Å, suprisely, the total minimum energy of -226.672 Ry, was higher than when the hydrogen atom is attached to sulphur.

   From the above, we can conclude that dissociation of H_2S is not favoured on Au clusters. The dissociation can occur only at the expense of energy.

Chapter 4

4 Conclusion and Summary

Using *ab initio* DFT calculation, based on ultra-soft pseudo-potential and PBE exchange-correlation, we have investigated the adsorption of H_2S molecules on neutral gold clusters Au_n(n=1-5).

It has been shown that H_2S molecules easily gets adsorbed on to the gold cluster. The adsorption energy for the the cluster decreases with increasing cluster size, this fact is also reflected in an elongation of Au-S bond.

In our simulation we discovered that the geometrical shapes of the gold cluster are more or less the same before and after adsorption of H_2S molecules. The structure of gold cluster remain planar (close to each other and on the same plane). The adsorbed molecules get adjusted in a way that their centers of mass lie on the plane of the gold cluster. We found that the lowest energy structure of the gold-molecule adsorbate results from the adsorption of the molecules on the lowest energy structure of the respective bare gold cluster. In all the cases considered, the adsorbed molecules get attached to a single gold atom and there is no preference to get adsorbed in between the gold.

From our result it became obvious that Au_2H_2S is more stable than their fragments and dissociation of H_2S is not favoured.

REFERENCES

[1] Q. Sun, Q. Wang, B. K. Rao, and P. Jena, Phys. Rev. Lett. 93, 186803 2004.

[2] H. Hakkinen, R. N. Barnett, and U. Landman, Phys. Rev. Lett. 82, 3264 1999.

[3] C. Majumder, T. M. Briere, H. Mizuseki, and Y. Kawazoe, J. Chem, Phys. 117, 2819 2002.

[4] R. Roussean and D. Marx, J. Chem. Phys. 112, 761 2000.

[5] A. Sanchez, S. Abbet, U. Heiz, W. D. Schneider, H. Hkkinen, R. N.Barnett, and U. Landman, J. Phys. Chem. A 103, 9573 1999.

[6] F. Boccuzzi and A. Chiorino, J. Phys. Chem. B 104, 5414 2000.

[7] L. M. Molina and B. Hammer, Phys. Rev. Lett. 90, 206102 2003.

[8] I. L. Garzon, J. A. Reyes-Nava, J. I. Rodriguez-Henndez, I. Sigal, M. R. Beltrn, and K. Michaelian, Phys. Rev. B 66, 073403 2002.

[9] C. E. Roman-Velazquez, C. Noquez, and I. L. Garzn, J. Phys. Chem. B 107, 12035 2003.

[10] H. Hakkinen and U. Landman, Phys. Rev. B 62, R2287 2000

[11] K. Sugawara, F. Sobott, and A. B. Vakhtin, J. Chem. Phys. 118, 7808 2003.

[12] X. Ding, Z. Li, J. Yang, J. G. Hou, and Q. Zhu, J. Chem. Phys. 121, 2558 2004.

[13]A. Sanchez, S. Abbet, U. Heiz, W. D. Schneider, H. Hkkinen, R. N. Barnett, and U. Landman, J. Phys. Chem. A 103, 9573 1999.

[14] J. Wang, G. Wang, and J. Zhao, Phys. Rev. B 66, 035418 2002.

[15]S. A. Varganov, R. M. Olson, M. S. Gordon, G. Mills, and H. Metiu, J. Chem. Phys. 120, 5169 2004.

[16] A. Calzolari, C. Cavazzoni, and M. Buongiorno Nardelli, Phys. Rev. Lett. 93, 096404 (2004).

[17] S. Gilb, P. Weis, F. Furche, R. Ahlrichs, and M. M. Kappes, J. Chem.

[18] H. Sellers, A. Ulman, Y. Shnidman, and J. E. Eilers, J. Am. Chem. Soc.115, 9389 1993.

[19] K. M. Beardmore, J. D. Kress, A. R. Bishop, and N. Grnboch-Jensen, Synth. Met. 84, 317 1997.

[20] C. Majumder, T. M. Briere, H. Mizuseki, and Y. Kawazoe, J. Chem. Phys. 117, 7669 2002.

[21] D. Krger, H. Fuchs, R. Rousseau, D. Marx, and M. Parrinello, J. Chem. Phys. 115, 4776 2001.

[22A] K. Sugawara, F. Sobott, and A. B. Vakhtin, J. Chem. Phys. 118, 7808 2003.

[22] S. A. Varganov, R. M. Olson, M. S. Gordon, G. Mills, and H. Metiu, J. Chem. Phys. 120, 5169 2004.

[23] A. A. Bagaturyant, A. A. Safonov, H. Stool, and H.-J. Werner, J. Chem. Phys. 109, 3096 1998.

[24] C. Majumder, T. M. Briere, H. Mizuseki, and Y. Kawazoe, J. Chem. Phys. 117, 2819 2002

[25] Y. Yu, St. J. Dixon-Warren, and N. Astle, Chem. Phys. Lett. 312, 455 1999 and references therein.

[26] A. G. Baca, M. A. Schulz, and D. A. Shirley, J. Chem. Phys. 81, 6304 1984.

[27] K. T. Leung, X. S. Zhang, and D. A. Shirley, J. Phys. Chem. 93, 6164 1989

[28] B. Fruhberger, M. Grunze, and D. J. Dwyer, J. Phys. Chem. 98, 609 1994.

[29] V. Bondzie, St. J. Dixon-Warren, and Y. Yu, J. Chem. Phys. 111, 10670 1999.

[30] D. M. Jeffey and R. J. Madix, Surf. Sci. 258, 359 1991.

[31] K. M. Beardmore, J. D. Kress, A. R. Bishop, and N. Grnbech-Jenson, Synth. Met. 84, 317 1997.

[32] Theory of the Inhomogeneous Electron Gas, eds. S. Lundqvist and N.H. March (Plenum, New York, 1983).

[33] Many-Body Phenomena at Surfaces, eds. D. Langreth and H. Suhl (Academic, New York, 1984) sets. I and II.

[34]P I Density Functional Methods in Physics, eds. R.M. Dreizler and J. da Providencia (Plenum, New York, 1985).

[35] The Electronic Structure of Complex Systems, eds. P. Phariseau and W.M. Temmerman (Plenum, New York, 1984).

[36] W.E. Pickett, Solid State Phys. 12 (1985) 1, ibid. 12 (1986) 57.

[37] T.L. Gilbert, Phys. Rev. B12 (1975) 2111.

[38] M. Berrondo and Goscinski, Intl. J. Quant. Chem. Symp. 9 (1975) 67.

[39] M. Levy, Proc. Natl. Acad. Sci. USA 76 (1979) 6062.

[40] J.F. Janak, Solid State Commun. 20 (1976) 151.

[41] U. von Barth and C.D. Gelatt, Phys. Rev. B21 (1980) 2222.

[42] D. Ceperley and B. Alder. Phys. Rev. Lett., 45:566, 1980.

[43] J. P. Perdew and A. Zunger. Phys. Rev. Lett., B23:5040, 1981.

[44] M. Schluter D. R. Hamann and C. Chiang. Phys. Rev. Lett., 43(1979), 1994.

[45] D. Vanderbil. Phys. Rev. B, 41:7892, 1990.

[46] Introduction of Quantum Mechanics. Prentice Hall, Inc Upper Saddle river, NJ07458, 1995.

[47] W.G. Hagos and Anjali Kshirsagar Chem. Phys 126, 244705 (2007)